Outgassing of Oxygen from Polycarbonate

Sung In Moon, L. Monson, and C. W. Extrand*

Entegris, Inc., 3500 Lyman Boulevard, Chaska, Minnesota 55318

ABSTRACT A manometric permeation apparatus was used to study the "outgassing" or desorption of oxygen from polycarbonate (PC). A PC film was placed in the apparatus. Both sides were exposed to oxygen until the film was saturated. To simulate inert gas purging of a closed container or "microenvironment", oxygen was pumped from one side of the apparatus to reduce the concentration on that side to nearly zero. Oxygen concentrations on the freshly purged side rose quickly at first but then slowed. Eventually, a steady state was established and oxygen concentrations increased linearly with time. Mass-transport coefficients (permeation, diffusion, and solubility coefficients) were also estimated and then used to successfully predict the postpurge rise of the oxygen concentration.

KEYWORDS: outgassing • desorption • permeation • diffusion • oxygen • polycarbonate

INTRODUCTION

Polycarbonate (PC) containers or "microenvironments (MEs)" are used widely in semiconductor fabrication facilities to protect and transport high-purity silicon as it is converted from raw wafers to integrated circuits. Today, some semiconductor manufacturing technologies have advanced to the point where previously benign constituents, such as water and oxygen, can be detrimental (1, 2). Purging with an inert gas is one method for lowering the water or oxygen levels inside the MEs. However, water or oxygen can "outgas" or desorb from the MEs, causing levels to quickly rise. For example, after an inert gas purge, the relative humidity inside a traditional PC wafer ME can climb to >30% over several hours. In the future, MEs will be required to maintain low oxygen and humidity levels for many hours.

We believe that much of this postpurge rise is due to desorption or "outgassing" from the materials of construction. In order to develop a fundamental understanding of this behavior so that we can create solutions, we have used permeation equipment to study outgassing of oxygen from PC. The upstream portion of the equipment represents the external environment, and the downstream side represents the inside of a ME. We attempted to replicate the postpurge concentration rise observed in MEs by first saturating a specimen with oxygen and then briefly pumping downstream side. After this short purge, the oxygen concentration was monitored over time.

ANALYSIS

Gas Concentrations within the PC. Figure 1 depicts a sample configured for either a standard time-lag permeation test or an outgassing simulation. Both assume one-dimensional gas transport through a film of uniform thickness (B). The two tests differ in the initial concentration

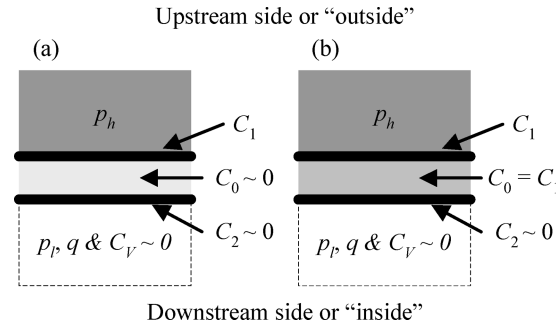

FIGURE 1. Cross-sectional depictions of a sample at the start of either (a) a standard time-lag permeation test or (b) an outgassing simulation.

within the bulk (C_0) of the PC. At the start of a permeation test, the PC is free of oxygen, $C_0 \sim 0$ (Figure 1a). The upstream face of the PC film is in contact with oxygen gas at a pressure of p_h. The corresponding concentration of gas in the PC at the upstream interface is C_1. The pressure on the downstream side (p_l) is effectively zero. Therefore, the concentration of oxygen gas dissolved in the PC downstream interface is zero, $C_2 \sim 0$. As the test proceeds, the sharp gradient at the upstream interface drives oxygen gas across the PC film. During the earliest stages of a permeation test, p_l does not change appreciably. It lags because a finite amount of time is required for the gas to reach the downstream interface. As the gas breaks through, p_l begins to increase. At longer times, a steady state usually is established, where p_l increases linearly with time.

Figure 1b shows the pressures and concentrations at the instant that an outgassing simulation begins. The upstream or "outside" pressure (p_h) remains constant. After an instantaneous purge of the downstream or "inside" volume, $p_l \sim 0$. Accordingly, the concentration of the oxygen gas at the upstream or "outer" surface of PC is C_1, whereas on the downstream side or "inside", it is effectively zero, $C_2 \sim 0$. In contrast to the permeation test, at the beginning of an outgassing simulation, the PC contains dissolved oxygen, $C_1 = C_0$. The sharp concentration gradient is now at the downstream interface, and gas immediately begins to des-

* Tel: 952-556-8619. E-mail: chuck_extrand@entegris.com.
Received for review March 26, 2009 and accepted June 3, 2009

DOI: 10.1021/am900206e

ARTICLE

orb or outgas from the PC film. With the passage of time, the rise of p_l slows and eventually reaches a steady-state condition.

Quantifying Permeant Volume and Concentration. The downstream pressure (p_l) of the permeant can be converted to an equivalent volume of gas (q) at standard temperature and pressure (STP)

$$q = \frac{p_l}{p_0}\frac{T_0}{T}V \tag{1}$$

where T is the measurement temperature, V is the volume of the downstream side of the permeation apparatus (V = 341.8 cm^3), T_0 is the standard temperature (0 °C = 273 K), and p_0 is the standard pressure (1 atm = 76 cmHg). It is useful to convert this volume of gas q into a concentration (C_V) contained by the downstream volume or the volume inside the isolated ME (V)

$$C_V = \frac{q}{V} \tag{2}$$

Estimating Mass-Transport Coefficients. Mass-transport coefficients were estimated using the time-lag technique. This standard permeation test method, which has been used widely to evaluate polymers (3), was pioneered by Daynes (4) and Barrer (5). The analysis assumes that the upstream pressure, p_h (and C_1), remains constant over time and $p_h > p_l$ ($C_1 > C_2$). At the start of the test, the film is gas-free and $p_l \sim 0$ ($C_0 = C_2 \sim 0$). Gases permeate through polymers by first adsorbing and then diffusing. A diffusion coefficient (D) can be calculated from the lag or breakthough time (t_b) and the film thickness (B) (6),

$$D = \frac{B^2}{6t_b} \tag{3}$$

During the latter stages of the time-lag test, a steady state is established and q increases linearly with time (t). A permeability coefficient (P) can be determined from the slope (q/t) of this linear portion

$$P = \frac{B}{Ap_h}\frac{q}{t} \tag{4}$$

where B is the film thickness, A is the film area, and p_h is the applied upstream pressure (3−7). A solubility coefficient (S) can be estimated from the quotient of the permeability and diffusion coefficients

$$S = \frac{P}{D} \tag{5}$$

Predicting Outgassing. The postpurge rise of the concentration (C_V) inside a "ME" of volume V can be estimated as (5)

$$C_V = \frac{A}{V}\left\{D(C_1 - C_2)\frac{t}{B} + \frac{2B}{\pi^2}\sum_{n=1}^{\infty}\frac{C_1\cos n\pi - C_2}{n^2}[1 - \exp(-Dn^2\pi^2 t/B^2)]\right\} + \frac{A}{V}\left\{\frac{4C_0B}{\pi^2}\sum_{m=0}^{\infty}\frac{1}{(2m+1)^2}[1 - \exp(-D(2m+1)^2\pi^2 t/B^2)]\right\} \tag{6}$$

where C_0 and C_1 come from the solubility coefficient and the upstream or external pressure of the gas

$$C_0 = C_1 = Sp_h \tag{7}$$

and C_2 is the product of the solubility coefficient and the time-dependent downstream pressure

$$C_2 = Sp_l \tag{8}$$

EXPERIMENTAL DETAILS

The oxygen gas used in both the permeation and outgassing measurements was of industrial grade from Toll Co., Minneapolis, MN. Extruded PC films having thicknesses (B) of 0.25 and 0.51 mm were obtained from Sabic (8010-MC-112). According to the supplier, the films were extruded from Lexan 141 Bisphenol A PC resin. They were dense, clear, colorless, and amorphous, containing no additives, fillers, or porosity. The melt flow rate of the extruded films was 9.3 dg/min (300 °C, 1200 g load). We measured a glass transition temperature of 148 °C by differential scanning calorimetry. (No melting point was observed.) The films were used as received without further treatment.

The permeation/outgassing apparatus, shown in Figure 2, was constructed from stainless steel components and consisted of a sample holder inside a temperature-controlled chamber, a series of valves, a 1 L upstream ballast tank, a pressure transducer (300 psi Heise PM digital indicator) for the upstream gas, a 300 mL downstream receiving tank, and a downstream solid-state manometer (10 Torr MKS Baratron type 627B). Connections were made by welding or with VCR flanges to minimize leaks. Data acquisition and control were performed remotely with a personal computer. The upstream pressure (p_h) and temperature were monitored over the duration of all experiments to ensure their constancy. Measurements were performed using three upstream gas pressures (0.2, 0.5, and 1.0 atm). All measurements were made at T = 25 °C (77 °F).

Permeation was measured according to standard manometric procedures (4, 5, 8), as described below. A circular PC specimen with a diameter of 4.6 cm and an effective area (A) of 13.7 cm^2 was placed in the apparatus. The entire apparatus was pumped down to approximately 2×10^{-3} cmHg and held there to remove gas and volatile constituents from the apparatus as well as from the specimen. After pump down and degassing, the apparatus was leak tested. If the leak rate was sufficiently low, then the upstream side of the apparatus was charged with oxygen gas. The pressure and temperature were allowed to equilibrate for a few minutes, and then the permeation test was started. The downstream pressure (p_l) was recorded with the passage of time (t).

For the outgassing measurements, a PC specimen was placed in the apparatus and pumped down. After sufficient degassing, both the upstream and downstream of the apparatus were

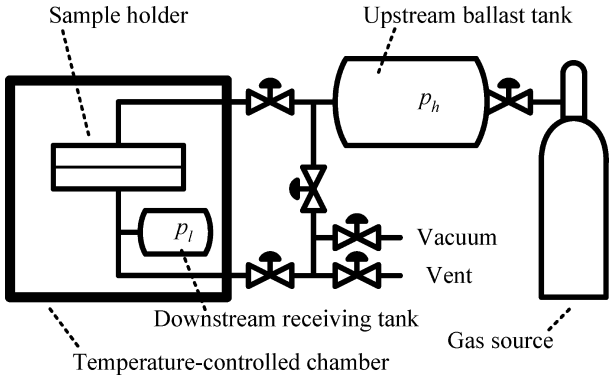

FIGURE 2. Schematic depiction of the permeation/outgassing apparatus. (Components are not depicted with actual dimensions or proportions.)

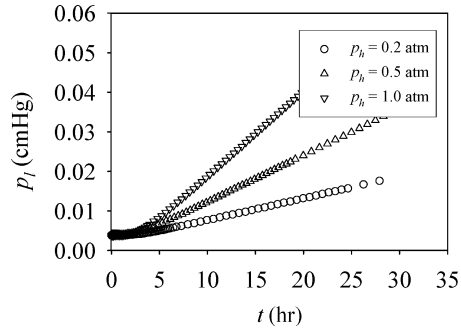

FIGURE 3. Downstream pressure (p_l) versus time (t) from a permeation test.

charged with oxygen, exposing both faces of the specimen to the permeant. The specimen was left in contact with oxygen for sufficient time to allow complete saturation throughout the PC. This soak time varied between 24 and 48 h, depending on the thickness of the specimen. To simulate the purging of a ME, oxygen gas then was pumped from the downstream volume (V) of the apparatus. When the concentration of the downstream side had been reduced to the desired level, the downstream valve was closed to initiate the outgassing test. The downstream pressure (p_l) was recorded with the passage of time (t).

The downstream volume was isolated from the vacuum at the start of both permeation and outgassing measurements. Pumping during an experiment would have removed any oxygen gas that had permeated through or desorbed from the PC film, erroneously lowering the measured p_l values. For these types of measurements, it is essential that the leak rate is sufficiently low that it does not significantly contribute to p_l. The leak rate of this system typically was 2×10^{-8} cmHg/s (=8×10^{-8} cm^3/s at STP). The longest experiments were 50 h. Therefore, the total increase in p_l due to leakage at the end of the longest experiments was 4×10^{-3} cmHg (or 1×10^{-2} cm^3 at STP), which corresponds to a leakage error in p_l (or q or C_V) of <1 %.

RESULTS AND DISCUSSION

Permeation Measurements and Mass-Transport Coefficients. Figure 3 shows an example of raw data for several permeation measurements. The data were obtained from a 0.51-mm-thick PC specimen exposed to three different upstream pressures, p_h = 0.2, 0.5, and 1.0 atm. These upstream pressures correspond to 15, 38, and 76 cmHg. Initially, the downstream pressure did not increase until oxygen reached the downstream side. Note that the lag time from the three different pressures was the same. Once oxygen broke through, the downstream pressure increased at a rate proportional to the upstream pressure. Thus, the greater the upstream pressure, the faster the rise of oxygen downstream.

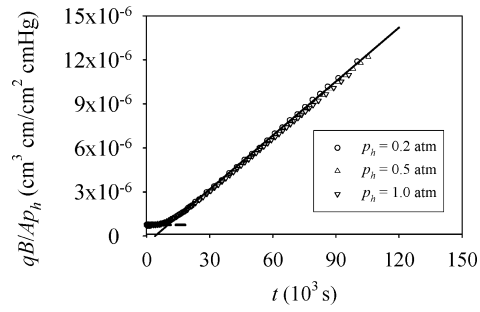

FIGURE 4. Plot of qB/Ap_h versus time (t), according to eq 4.

Table 1. Oxygen Permeability Coefficients (P), Diffusion Coefficients (D), and Solubility Coefficients (S) for PC[a]

Origin of data	P (10^{-10} cm^3 · cm/cm^2 · s · cmHg)	D (10^{-8} cm^2/s)	S (10^{-3} cm^3/cm^3 · cmHg)
this work	1.2 ± 0.1	3.8 ± 0.2	3.3 ± 0.1
Norton (ref 9)	1.4	2.1	0.51
Haraya and Hwang (ref 10)	1.2	2.9	4.1
Gao, Baca, Wang, and Ogilby (ref 11)		5.5	
Kim, Aguilar-Vega, and Paul (35 °C, ref 12)	1.6	7.0	2.5
Chen, Huang, Yu, Lai, and Liang (35 °C, ref 13)	1.5		3.3

[a] Unless noted otherwise, measurements were made at 25 °C.

These data can be rearranged using eq 4 to calculate the permeation properties. The results are shown in Figure 4. The points are experimental data. The solid line represents linear regression for longer times. The slope of the line is equal to the permeability coefficient (P), which has a value of $P = 1.2 \times 10^{-10}$ cm^3 · cm/cm^2 · s · cmHg. The breakthrough or lag times (t_b) were estimated from the intersection of two lines: the first is defined by the permeability coefficient, and the second is a zero-slope dashed line passing through the initial p_l at t = 0 s. For the data in Figure 4, t_b = 11 000 s (about 3 h), corresponding to a diffusion coefficient of $D = 3.8 \times 10^{-8}$ cm^2/s. From the quotient of P and D (eq 5), the solubility coefficient was estimated as $S = 3.3 \times 10^{-3}$ cm^3/cm^3 · cmHg. If analyzed individually, data from each of the pressures gave nearly identical values of P, D, and S.

Other trials behaved similarly. The permeation rates were proportional to the applied upstream pressure and inversely proportional to the thickness. The data from various pressures and thicknesses gave unique values of P, D, and S. Table 1 lists the overall averages of mass-transport coefficients from our permeation tests along with data from other investigators (9−14). Even though the PC used by various investigators came from different suppliers, the specimens were prepared with different methods (solvent casting versus extrusion) and the specimens were tested with different techniques (manometric versus spectro-

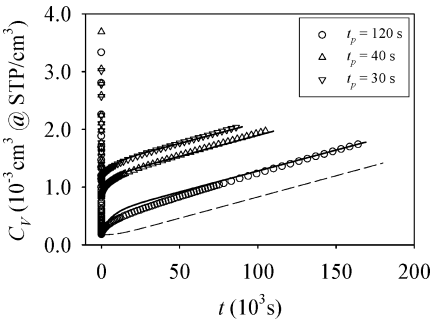

FIGURE 5. Downstream concentration (C_V) of oxygen versus time (t) for $B = 0.51$ mm thick PC after various pump-down times (t_p). The PC specimen was conditioned and tested with $p_h = 1.0$ atm. The symbols are experimental data. The solid lines are predicted outgassing values based on eq 6. The dashed line shows the predicted permeation behavior, assuming that the PC was initially nearly free of oxygen.

scopic); the results generally agreed well. The P values measured at 25 °C were within 20% of each other. The P values measured at 35 °C were slightly higher. The D values ranged from 2.1×10^{-8} to 7.0×10^{-8} cm^2/s. Our D value fell in the middle of these. With the exception of the data of Norton, the S values resided within a relatively narrow band, $(2.5-4.1) \times 10^{-3}$ cm^3/cm$^3 \cdot$cmHg. (It is not clear how Norton arrived at an S value of 0.51×10^{-3} cm^3/cm$^3 \cdot$cmHg. An estimate of S from his P and D values is 6.7×10^{-3} cm^3/cm$^3 \cdot$cmHg, which is an order of magnitude greater than the value listed in his paper.)

Outgassing Measurements. Figure 5 shows the downstream concentration (C_V) of oxygen versus time (t) for a 0.51-mm-thick PC after various pump-down times (t_p). The symbols are experimental data. The upstream pressure was $p_h = 1.0$ atm $= 76$ cmHg. The downstream pressures (p_l) were converted into concentrations via eqs 1 and 2. These concentrations, plotted on the vertical axis, have units of cm^3/cm^3, where the numerator is a gas volume at standard temperature and pressure (STP) and the denominator is the unit volume of the downstream side or "inside" our model ME.

The three pump-down times showed the same general behavior. The concentration of oxygen gas on the downstream side (C_V) fell rapidly during the pump down. The pump-down times, which ranged from $t_p = 30$ to 120 s, reduced the initial oxygen concentration in the model ME to $(0.1-1) \times 10^{-3}$ cm^3/cm^3. Thus, the starting concentration for these outgassing experiments is less than or equal to 0.1% of the original conditioning concentration in the system (0.92 cm^3/cm^3). As expected, longer "purging" produced lower initial concentrations. When the pump down was stopped to begin the outgassing test, C_V rose rapidly at first because of oxygen desorbing from the immediate surface of the PC.

As time passed, C_V increased more slowly. Oxygen from "outside the ME" continually replenished oxygen that had outgassed into the "ME". Eventually, a steady state was established and the concentration in the downstream volume (C_V) increased linearly with time. The C_V values ultimately climbed to several parts per thousand (ppt) in a day.

The test durations were 24−48 h. Establishing a steady state for the 0.51-mm-thick PC specimen took roughly 9 h, about 3 times the breakthough time (t_b) from the permeation measurements. C_V increased linearly at longer times because $C_1 \gg C_2$ and $C_2 \approx 0$. If the test had been allowed to run for weeks such that the concentration on the inside PC layer of the "ME", C_2, was no longer much less than the concentration on the outside C_1, then the slope of C_V versus t would have begun to decline as C_2 approached C_1. If the upstream and downstream concentrations had reached equilibrium, such that $p_h = 1.0$ atm, C_V would have been 0.92 cm^3/cm^3.

The solid curves show the concentration rise calculated from eqs 6−8 using measured D and S values found in Table 1. The agreement between the measured and predicted values was generally quite good. After the longest purging time, the calculation slightly overestimated the early stages of outgassing. Why? Equation 6 assumes that the concentration of oxygen dissolved in the PC (C_0) is constant across the thickness of the film and remains constant during pump down. From the experimental perspective, this is equivalent to an instantaneous purge. With our experimental setup, pump down was not instantaneous: tens of seconds were required to sufficiently reduce the downstream concentration. While pump-down times of $t_p = 30$ or 40 s did not appreciably reduce C_0, it appears that longer times did. For $t_p = 120$ s, it is likely that a reduced C_0 led to an overestimation of C_V at the early stages of outgassing.

One can approximate the average depletion by changing C_0 in eq 6. Reducing C_0 by 10% greatly improved the fit of the data for $t_p = 120$ s. However, this is a crude estimate. The concentration would not be depleted uniformly across the thickness of the PC but would be most pronounced at the inner surface, with little or no change in C_0 throughout the remainder of the specimen. Including a more realistic concentration profile would further complicate an already complex analysis.

Figure 5 also includes the predicted behavior if the PC specimen were initially free of oxygen, where the rise in C_V would have been driven solely by permeation from the upstream side or "outside". This permeation is depicted by the dashed curve. It also was estimated using eq 6, where the initial concentration in the PC was assumed to be zero, $C_0 \sim 0$. Note that the steady-state portions of the outgassing and permeation curves have the same slope but are offset by the amount of outgassed oxygen. In Figure 5, the concentration rise due to desorption alone was $\sim 4 \times 10^{-4}$ cm^3/cm^3.

Equation 6 assumes that both C_1 and C_2 are constant; it was not derived to accommodate a time-dependent concentration on either side. In our case, the upstream concentration (C_1) remained constant. The concentration on the downstream (C_2) side started low and did not become too high during our measurements. As compared to C_1, C_2 was effectively zero. For our experiments, C_2/C_1 was always <0.5%. Therefore, using eq 6 to describe our data is a reasonable approximation.

Figure 6 shows the downstream concentration (C_V) of oxygen versus time (t) for the $B = 0.51$ mm thick PC specimen that was conditioned and tested with three different upstream pressures, $p_h = 0.2$, 0.5, and 1.0 atm. Note that $p_h = 0.2$ atm roughly equates to the oxygen levels found in ambient air. (At $p_h = 0.2$ atm, equilibrium C_V would be

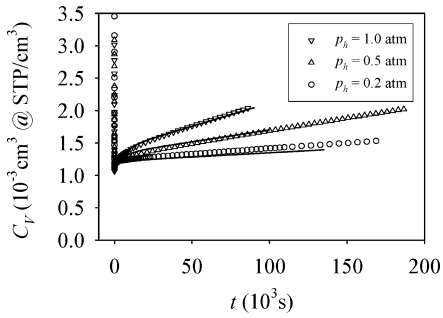

FIGURE 6. Downstream concentration (C_V) of oxygen versus time (t) for the $B = 0.51$ mm thick PC specimen that was conditioned and tested with $p_h = 1.0$, 0.5, and 0.2 atm. The pump-down time for these trials was $t_p = 30$ s. The symbols are experimental data. The solid lines are predicted values based on eq 6.

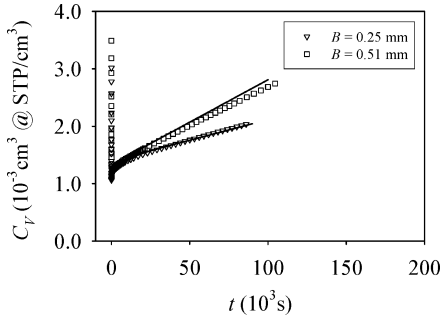

FIGURE 7. Downstream concentration (C_V) of oxygen versus time (t) for PC specimens that had two different thicknesses, $B = 0.25$ and 0.51 mm. Both thicknesses were conditioned and tested with an upstream pressure of $p_h = 1.0$ atm. The pump-down time (t_p) was 30 s. The symbols are experimental data. The solid lines are predicted values based on eq 6.

0.18 cm^3/cm^3.) The pump-down time for these trials was $t_p = 30$ s, which yielded C_V of 1×10^{-3} cm^3/cm^3 at $t = 0$ s. C_V values rose rapidly at first and then slowed. The initial rise of C_V increased with p_h and so did the steady-state region observed at longer times. Here, C_V was proportional to p_h. The steady-state slope (C_V/t) of $p_h = 0.5$ atm was 2.5 times that of $p_h = 0.2$ atm; the slope of $p_h = 1.0$ atm was 5 times greater.

Figure 7 shows the downstream concentration (C_V) of oxygen versus time (t) for PC specimens that had two different thicknesses, $B = 0.25$ and 0.51 mm. Both thicknesses were conditioned with an upstream pressure of $p_h = 1.0$ atm. The pump-down time was $t_p = 30$ s. Again, C_V climbed rapidly followed by a decline toward a steady state. At the beginning, the two curves are nearly indistinguishable. All else being equal, the thickness of the specimen is relatively unimportant at the earliest stages. Oxygen desorbing from the immediate surface of the downstream side or "inside the ME" drove the increase in C_V. As the two thicknesses established a steady state at longer times, they diverged. Here, oxygen that had permeated from the upstream side began to contribute to the observed outgassing. Accordingly, the thicker sample climbs at half the rate of the thinner one.

The P values can also be extracted from outgassing experiments. The average value from the steady-state portion of the curves in Figures 5–7 was nearly identical with the average P values from the standard permeation tests. This study focused on oxygen, but the experimental techniques and models employed here can be used for a wide assortment of gases and vapors, including water vapor and volatile organic compounds.

CONCLUSIONS

We were able to successfully simulate the postpurge oxygen concentration rise observed in MEs using a gas permeation apparatus. To prepare for an outgassing test, a PC specimen was saturated by exposing both sides to oxygen. Next, oxygen was removed from the downstream side with a vacuum pump. When the pressure was reduced to a sufficiently low level, the test was initiated. In the early stages, the downstream or "ME" concentration (C_V) rose rapidly. At longer times, a steady state was established and C_V increased linearly with time. The extent of postpurge outgassing depended on the pump-down time, gas pressure (or concentration), and material thickness. Increasing the pump-down or "purge" time reduced the initial C_V value, effectively shifting the outgassing curves downward. Increasing the upstream pressure (p_h) led to greater outgassing. All else being equal, the thickness of the specimen was relatively unimportant at the earliest stages. However, at longer times, C_V increased at rates that were inversely proportional to the specimen thickness. Over the course of a typical outgassing test, "postpurge" oxygen concentrations climbed from zero to several parts per thousand (ppt) in a day. Diffusion and solubility coefficients measured as part of this study were used to successfully predict the outgassing-driven rise of oxygen.

Acknowledgment. We thank the Entegris, Inc., management for supporting this work and allowing publication. Also, thanks go to B. Arriola, E. Adkins, S. Cantor, C. Duston, J. Goodman, T. King, S. Moroney, J. Pillion, S. Sirignano, S. Tison, and B. Waldridge for their suggestions on the technical content and text.

REFERENCES AND NOTES

(1) Shrive, L. W.; Blank, R. E.; Lamb, K. H. *Micro* **2001**, *19*, 59.
(2) Extrand, C. *Semicond. Fabtech* **2008**, *3*, 43.
(3) Vieth, W. R. *Diffusion in and through Polymers*; Hanser: New York, 1991.
(4) Daynes, H. A. *Proc. R. Soc. London, Ser. A* **1920**, *97*, 286.
(5) Barrer, R. M. *Diffusion in and through Solids*; Cambridge University Press: New York, 1951.
(6) Crank, J. *The Mathematics of Diffusion*; Oxford University Press: London, 1970; Chapter 4.
(7) Osswald, T. A.; Menges, G. *Materials Science of Polymers for Engineers*; Hanser: New York, 1995; Chapter 12.
(8) *Standard Test Method for Determining Gas Permeability Characteristics of Plastic Film and Sheeting*; American Society for the Testing of Materials: West Conshohocken, PA, 1998; ASTM D1434-82. *Test Method for Gas Transmission Rate through Plastic Film and Sheeting*; Japanese Industrial Standard: Tokyo, Japan, 1987; JIS K7126.
(9) Norton, F. J. *J. Appl. Polym. Sci.* **1963**, *7*, 1649.
(10) Haraya, K.; Hwang, S.-T. *J. Membr. Sci.* **1992**, *71*, 13.
(11) Gao, Y.; Baca, A. M.; Wang, B.; Ogilby, P. R. *Macromolecules* **1994**, *27*, 7041.
(12) Kim, C. K.; Aguilar-Vega, M.; Paul, D. R. *J. Polym. Sci., Part B: Polym. Phys.* **1992**, *30*, 1131.
(13) Chen, S.-H.; Huang, S.-L.; Yu, K.-C.; Lai, J.-Y.; Liang, M.-T. *J. Membr. Sci.* **2000**, *172*, 105.
(14) Chen, S.-H.; Ruaan, R.-C.; Lai, J.-Y. *J. Membr. Sci.* **1997**, *134*, 143.

AM900206E